Independent Component Analysis of Mixels in Agricultural Land Using An Airborne Hyperspectral Sensor Image

Naoko KOSAKA[*1], Masao SHIMOZATO[*2], Kuniaki UTO[*3], and Yukio KOSUGI[*4]

[*1, 2, 3, 4] Tokyo Institute of Technology, 4259, Nagatsudacho, Midori-ku, Yokohama-shi, 226-8502, JAPAN
[*1] d02kosaka@pms.titech.ac.jp [*2] m02shimozato@pms.titech.ac.jp [*3] uto@pms.titeach.ac.jp [*4] kosugi@pms.titech.ac.jp

Abstract: Satellite and airborne hyperspectral sensor images are suitable for investigating the vegetation state in agricultural land. However, image data obtained by an optical sensor inevitably includes mixels caused by high altitude observation. Therefore, mixel analysis method, which estimates both the pure spectra and the coverage of endmembers simultaneously, is required in order to distinguish the qualitative spectral changes due to the chlorophyll quantity or crop variety, from the quantitative coverage change.

In this paper, we apply our agricultural independent component analysis (ICA) model to an airborne hyperspectral sensor image, which includes noise and fluctuation of coverage, and estimate pure spectra and the mixture ratio of crop and soil in agricultural land simultaneously.

Keywords: ICA, Mixel Analysis, Hyperspectral Data.

1. Introduction

Satellite and airborne hyperspectral sensor images are suitable for investigating the vegetation state in agricultural land, such as the variety and growth stage of crops, effect of insects and disease damage, biochemical components included in crops, and so on, since the observation can be conducted widely, periodically and objectively. However, image data obtained by an optical sensor inevitably includes mixels caused by high altitude observation. Therefore, mixel analysis methods, which estimate both the pure spectra and the coverage of endmembers simultaneously, is required in order to distinguish the qualitative spectral changes due to the chlorophyll quantity, crop variety, or crop damage, from the quantitative coverage change.

Most conventional methods require the pure spectra or knowledge of objects to estimate the mixture ratio from an observed mixed data. Besides, several attempts using ICA[1], which does not need *a priori* knowledge of objects, have been reported to estimate mixture ratio and spectral absorption wavelength of objects. However, the canonical form of ICA could not been successfully applied to most vegetation owing to similarity of chlorophyll absorption property.

In this paper, we apply our agricultural ICA model[2][3][4] to an airborne hyperspectral sensor image, which includes noise and fluctuation of coverage, and estimate pure spectra and the mixture ratio of crop and soil in agricultural land simultaneously.

2. Procedure of ICA-Aided Mixel Analysis

Fig.1 shows an agricultural land observatory scheme using an airborne hyperspectral sensor. Mixel data sampled at position x is described as bellow,

$$I(\lambda,x)=I_0(\lambda)\cdot\{R_v(\lambda)\cdot\eta_v(x)+R_s(\lambda)\cdot\eta_s(x)\}. \quad (1)$$

Where $R_v(\lambda)$ and $\eta_v(x)$ are the pure spectra and the coverage of crops. $R_s(\lambda)$ and $\eta_s(x)$ are those of soil. $I_0(\lambda)$ is the intensity of incident light.

The scan direction should not be parallel to the ridge direction in order to analyze the periodical profile of coverage of vegetation and soil derived from ridges. The direction yielding the most significant non-Gausian independent component (IC) is the adequate scan direction among several directions tilting against the boundary of a field. Since the ridge direction is parallel to the field boundary, and the optimal ridge width in relation to the scan direction depends on the scan window size.

In our linear mixel analysis model for agricultural land using ICA[2][3][4], each parameter is interpreted as ICA parameter shown in Table 1. ICA enables us to estimate both the mixture ratio, reflectance, and independent components, coverage, simultaneously. As *a priori* knowledge in this paper, we applied the first derivatives of soil spectra derived from JHU spectral library[5].

We used the package of Fast ICA in MATLAB[6] opened to public in the experiment.

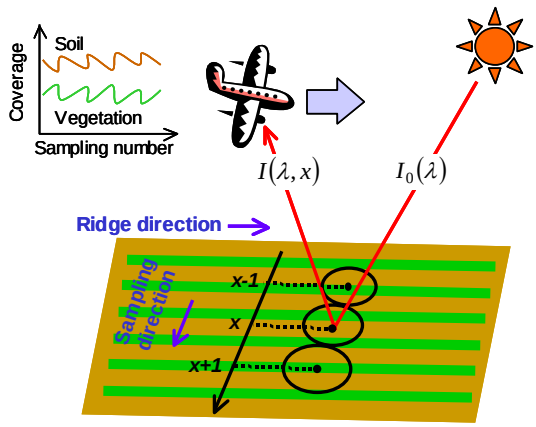

Fig.1 An observation of agricultural land.

Table 1 Parameters interpreted as ICA.

	in our method	in ICA
λ	wavelength	position of observation
x	center position of the circular window	time
$R_v(\lambda), R_s(\lambda)$	reflectance	mixture ratio
$\eta_v(x), \eta_s(x)$	coverage	independent component

3. Experiment

1) Target Vegetation

Fig.2 shows target vegetation called Japanese persimmon tree, which is a kind of fruit trees in Japan. Each tree is mostly same size and planted periodically as described in the sketch of the field in Fig.3. However, a few pumpkins are planted in parts of the field, it is ignorable due to infinitesimal size. The vegetation coverage of the filed is affected by the coverage inside of a crown. The coverage inside a crown, C_{crown}, is evaluated from the average value of four skyward photos for a certain typical tree as shown in Fig.4. Then we calculate an area size of a crown, S_{crown}, from the averaged radius of 8 directions for three trees as in Fig.5. Therefore, we derived the coverage of the field as,

$$C_{field} = C_{crown} \times S_{crown} \times N / S_{field} \ . \qquad (2)$$

Where N is the tree number in the field, and S_{field} is an area size of the field. Here, C_{field} is 53.4%.

Fig.2 Japanese persimmon tree.

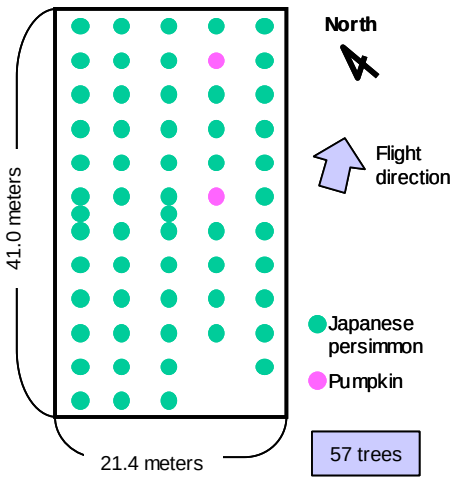

Fig.3 Sketch of the Japanese persimmon field.

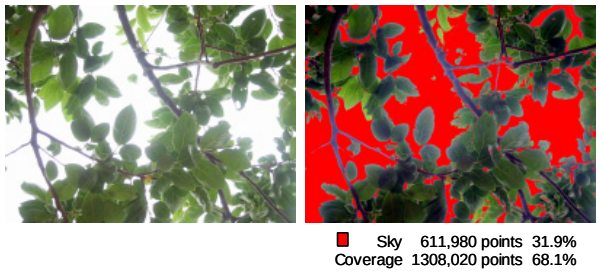

Fig.4 Coverage inside of a crown.

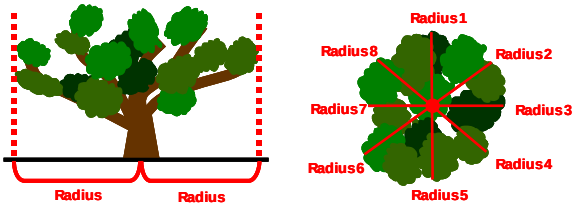

Fig.5 Crown radius.

2) Hyperspectral Data Acquisition

Table 2 shows a specification of the hyperspectral sensor, ImSpector V10, made by Spesim Co. In the preprocessing, 61 bands from 500 to 800nm range were used, and radiance value is transformed into reflectance applying empirical line method using the field spectra of artificial objects. The flight condition is shown in Table 3.

Table2 Specification of hyperspectral sensor.

Spectral Range	400-1000 nm
Band number	121 band
Spectral Resolution	3 nm
Sampling Interval	5 nm
Frame Rate	30 frames/sec
F number	4
Dynamic Range	10 bits

Table3 Condition of the flight.

Date	July 16, 2003
Time (J.S.T.)	12:00 p.m.
Weather	fine
Flight Hight	3000 feets
Flight Speed	73 m/sec

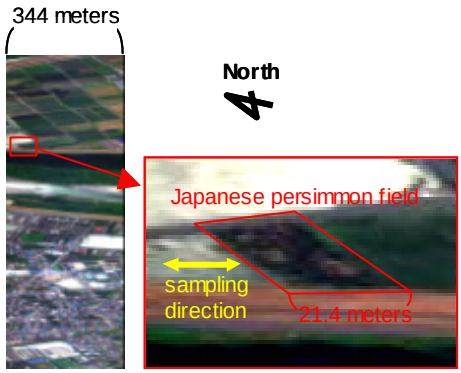

Fig.6 Hyperspectral image in true color.

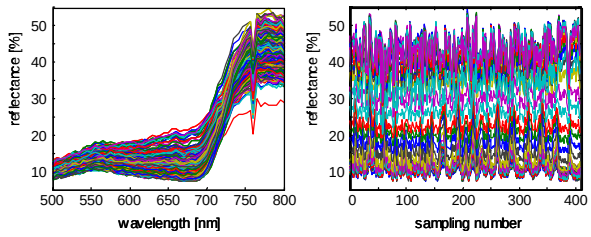

Fig.7 Spectral and periodical profiles of mixel data.

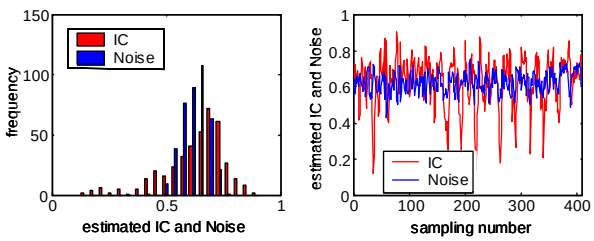

Fig.8 Density and periodical profile of estimated coverage.

A hyperspectral image of 344m in width is obtained with the resolution of 2.43m along the flight direction and 0.71m for across. Shapes of fields are not rectangle, because the flight direction is not parallel to the boundary of fields as shown in Fig.3 and Fig.6. In our experiment, row direction of detectors for push bloom sensor is set in the sampling direction, which is across to the flight direction. Fig.7 shows the mixel data input for ICA, which has 408 samples.

4.Results and Discussion

Estimated IC and noise are shown in Fig.8. Here, IC is the coverage of Japanese persimmon. Averaged IC is 62.3% and an error is +8.9% in coverage. Estimated spectra are shown in Fig.9. In Fig.9, image spectra are obtained from pixels, which are most pure area in a hyperspectral image. Mean and the maximum errors in a band are 3.4% and 8.8% for Japanese persimmon, and 3.0% and 9.1% for soil. Error in wavelength of visible range is a few percents. And error in wavelength of NIR is less than 10%. These errors resulted from differences of where each spectrum is obtained. The estimated spectra are averaged one for whole the field, while compared image spectra are derived from small area.

When compared with the field spectra, error was larger than those with image spectra as shown in Fig.10. As mentioned for image spectra, observed area size affected the results. For an accurate estimation, it is also necessary to make more precise transformation of reflectance.

5. Conclusions

In this paper, we applied our agricultural ICA model to the airborne hyperspectral sensor image. Our technique enabled to estimate both the pure spectra and the coverage for the Japanese persimmon tree field from a real remote sensing data, which includes noise and fluctuation of coverage.

As a future work, we will investigate the allowable sampling direction of mixed data, because the ridge direction is unknown in most mixel data. Moreover, in applying to narrower ridge width, we will have to remove blur effect by de-convolution.

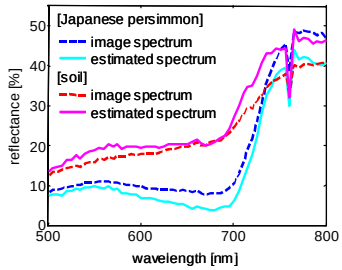

Fig.9 Estimated spectra and image spectra.

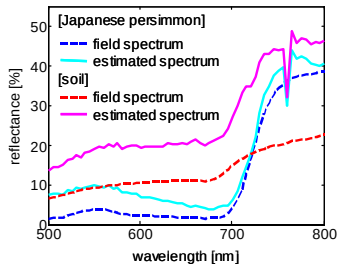

Fig.10 Estimated spectra and field spectra.

Acknowledgement

The authors thank Mr. S. Motohashi, Mr. M. Miyadera, Mr. M. Takano, K. Takano, and Ms. Y. Takasago for corporation to obtain the data of farmland. This work was partly supported by the Grant in Aid for Scientific Research #15100003.

References

[1] Parra, L. and Mueller, K. R. et al., 2000. Unmixing hyperspectral data , *Advances in Neural Information Processing Systems 12*, MIT Press, pp. 942-948.

[2] Kosaka, N. and Kosugi, Y., 2003. ICA aided linear spectral mixture analysis of agricultural remote sensing images, *Proc.ICA2003*, pp.221-226.

[3] Kosaka, N. and Shimozato, M. et al., 2003. Independent component analysis of periodically distributed hyperspectral mixel data for vegetation monitoring, *Proc. ISPRS WG VII-6.*

[4] Kosaka, N. and Shimozato, M. et al., 2003. Linear mixel analysis of hyperspectral data for vegetation monitoring, *Proc. ISPRS WG VII-6.*

[5] **URL:** Johns Hopkins University (JHU) Spectral Library at: http://asterweb.jpl.nasa.gov/speclib.

[6] **URL:** Oja, E. FastICA package for MATLAB at: http://www.cis.hut.fi/~aapo/pub.html#FastICA.